

# Time correlation functions via forward-backward quantum dynamics using Hamilton's law of varying action

Jonathan Chen and Nancy Makri<sup>a)</sup>*Department of Chemistry, University of Illinois, 601 S. Goodwin Avenue, Urbana, Illinois 61801, USA*

(Received 12 June 2009; accepted 20 August 2009; published online 23 September 2009)

We introduce a stable numerical procedure for solving Bohm's equations of motion to compute quantum trajectories in the forward-backward quantum dynamics (FBQD) formulation of zero-temperature time correlation functions. Rather than integrating the differential equations forward in time, our method is based on a series expansion of the quantum trajectory, exploiting Hamilton's law of varying action to determine the expansion coefficients. Because in FBQD the quantum trajectories generally are smooth and the quantum potential is well behaved, our method allows accurate determination of time correlation functions in strongly anharmonic bound systems over several oscillation periods. © 2009 American Institute of Physics. [doi:10.1063/1.3224494]

## I. INTRODUCTION

It has been shown by de Broglie,<sup>1</sup> Madelung,<sup>2</sup> and more thoroughly by Bohm,<sup>3,4</sup> that the quantum dynamical problem (i.e., the time-dependent Schrödinger equation) can be mapped exactly onto the time evolution of a fluid of particles obeying classical hydrodynamic equations of motion, with just one additional term accounting for all quantum effects on the classical fluid. Apart from its appeal as an exact alternative to Schrödinger's and Feynman's formulations of quantum mechanics, Bohm's trajectory description lends itself naturally to quantum-classical treatments, in which the trajectories would experience the quantum force only along those degrees of freedom that cannot be treated by classical mechanics.

In recent years, the quantum trajectory approach to dynamics has been pursued by several groups.<sup>5-27</sup> However, with the exception of a handful of favorable model systems, attempts to integrate Bohm's equations of motion exactly without recourse to conventional wavefunction methods have met with limited success, largely owing to the pathological behavior of the rugged quantum potential. If the quantum potential is neglected, the quantum trajectories are subject to the purely classical force. In that limit, Bohm's formulation reverts to the time-dependent semiclassical approximation, in which quantum mechanical effects are accounted for through the interference of classical trajectories that cross in coordinate space.<sup>21</sup> By contrast, Bohm's trajectories cannot cross. To prevent crossing, the quantum force acting on these trajectories must be sufficiently strong to alter the course of the particles dictated by the classical potential. As a consequence, the quantum force is often extremely large in magnitude and varies sharply with position. These features generally render numerical integration of Bohm's equations unstable.<sup>21</sup>

An attempt to alleviate this problem has been reported in the context of evaluating time correlation functions of posi-

tion or momentum operators at zero temperature. The forward-backward quantum dynamics (FBQD) formulation of time correlation functions<sup>28</sup> exploits the fact that these operators produce a near eigenstate of the Hamiltonian when acting on the ground state. Since the quantum trajectories emanating from eigenstates are straight lines, the near eigenstate that needs to be propagated backward in FBQD gives rise to very smooth trajectories governed by a well-behaved quantum potential, thus facilitating numerical solution. However, even in this very advantageous representation, integration of Bohm's equations of motion in bound anharmonic systems using conventional methods appears to be extremely challenging.

This paper explores an alternative to numerical integration of Bohm's differential equations. Section II reviews Bohm's formulation of quantum mechanics<sup>3,4</sup> and the FBQD method for computing zero-temperature time correlation functions.<sup>28</sup> Section III describes a variational approach, rooted in the analytical mechanics of Hamilton,<sup>29,30</sup> which seems to be free of the typical numerical sensitivity of the quantum potential at short times. Section IV illustrates this approach with two examples. A brief discussion and concluding remarks are given in Sec. V.

## II. BOHM'S FORMULATION AND FBQD

### A. Quantum trajectories from wavefunctions

For a one-dimensional particle in a potential field  $V_{cl}(x)$ , the evolution of the wavefunction is given by the time-dependent Schrödinger equation,

$$i\hbar \frac{\partial}{\partial t} \Psi(x,t) = -\frac{\hbar^2}{2m} \frac{\partial^2}{\partial x^2} \Psi(x,t) + V_{cl}(x) \Psi(x,t). \quad (2.1)$$

The starting point in Bohm's description is expression of the complex-valued wavefunction in amplitude-phase form,

$$\Psi(x,t) = R(x,t) \exp(iS(x,t)/\hbar), \quad (2.2)$$

where  $R(x,t)$  and  $S(x,t)$  are real-valued functions. Substitution of Eq. (2.2) into Eq. (2.1) and separation of real and

<sup>a)</sup>Electronic mail: nancy@makri.scs.uiuc.edu.

imaginary terms yield the quantum Hamilton–Jacobi equation,

$$\frac{\partial S(x,t)}{\partial t} + \frac{1}{2m} S'(x,t)^2 + V_{\text{cl}}(x) - \frac{\hbar^2 R''(x,t)}{2m R(x,t)} = 0 \quad (2.3)$$

(where primes indicate spatial derivatives), and an equation for the probability density  $\rho(x,t) \equiv R(x,t)^2$ ,

$$\frac{\partial \rho(x,t)}{\partial t} + \frac{1}{m} \frac{\partial}{\partial x} (\rho(x,t) S'(x,t)) = 0, \quad (2.4)$$

which is an Eulerian continuity equation for the flow of the probability density with the velocity given by the relation

$$p(x,t) = mv(x,t) = S'(x,t). \quad (2.5)$$

Taking the gradient of Eq. (2.3) and using the identity

$$\frac{d}{dt} = \frac{\partial}{\partial t} + v \frac{\partial}{\partial x} \quad (2.6)$$

yields a Newtonian equation of motion,

$$\frac{dp}{dt} + \frac{\partial}{\partial x} \left[ V_{\text{cl}}(x) - \frac{\hbar^2 R''(x,t)}{2m R(x,t)} \right] = 0. \quad (2.7)$$

Meanwhile, the Lagrangian version of the continuity equation is given by<sup>31</sup>

$$\rho(x_t, t) dx_t = \rho(x_0, 0) dx_0. \quad (2.8)$$

Equations (2.7) and (2.8) are Bohm's equations of motion in the particle-fixed (Lagrangian) frame. These equations govern the dynamics of a Bohmian fluid (or swarm of quantum trajectories) whose time evolution is fully equivalent to a solution of the Schrödinger equation (2.1). In this hydrodynamic picture, particle trajectories trace out the streamlines of the probability density  $|\Psi(x,t)|^2$  in configuration space, while the action integral yields the phase of the wavefunction along each trajectory.

Defining the quantum potential as

$$V_{\text{qm}}(x,t) = -\frac{\hbar^2 R''(x,t)}{2m R(x,t)}, \quad (2.9)$$

Eq. (2.7) can be written more suggestively as

$$\dot{p}(t) = -\frac{\partial}{\partial x} [V_{\text{cl}}(x) + V_{\text{qm}}(x,t)], \quad (2.10)$$

which is Newton's second law for a particle subject to the modified, time-dependent potential  $V_{\text{cl}}(x) + V_{\text{qm}}(x,t)$ . Thus, the presence of the quantum potential  $V_{\text{qm}}$  and the additional interparticle correlations implied by the continuity equation (2.8) are responsible for all deviations of the Bohmian particles from their classical trajectories.

Equations (2.7) and (2.8) provide an interesting conceptual framework for exact quantum mechanical propagation using trajectories, much in the spirit of classical mechanics. However, the quantum potential depends on collective properties of the quantum trajectories, reflecting the nonlocality of quantum mechanics. In practice, the ill-behaved nature of the rapidly varying quantum force in bound systems<sup>21</sup> usually causes numerical difficulties in the direct solution of Bohm's equations for the particle trajectories.

## B. Wavefunctions from quantum trajectories

Formal integration of the equations given in Sec. II A yields the information required to infer the time-dependent wavefunction,

$$\Psi(x_t, t) = \sqrt{\rho(x_t, t)} \exp[i(S_0(x_0) + S(x_t, t))/\hbar]. \quad (2.11)$$

In this expression the time-dependent density  $\rho(x_t, t)$  can be inferred from the continuity equation (2.8),  $S$  is the action integral of the full quantum Lagrangian  $L = T - (V_{\text{cl}} + V_{\text{qm}})$  (where  $T$  is the kinetic energy term) evaluated along the Bohmian trajectory from  $x_0$  to  $x_t$ , and  $\exp[iS_0(x_0)/\hbar]$  is the initial phase of the wavefunction at  $x_0$ . The latter determines the initial velocity field according to the relation

$$p_0(x_0) = S'_0(x_0), \quad (2.12)$$

which together with the density  $\rho(x_0, 0)$  specifies completely the initial conditions of the Bohmian particles. The latter are then moved forward in time according to Eqs. (2.8)–(2.10).

For example, when the initial state of the Bohmian problem is an eigenstate of the Hamiltonian, the Bohmian trajectories are simply given by straight lines, i.e.,  $x(t) = x_0$ . This is evident from the continuity relation and the fact that the probability density associated with an energy eigenstate (stationary state) does not vary with time.

## C. FBQD

The FBQD scheme exploits the structure of equilibrium correlation functions to tame the quantum potential. At zero temperature, the initial density operator is simply  $\hat{\rho}_0 = |\varphi_0\rangle\langle\varphi_0|$ , where  $|\varphi_0\rangle$  is the ground state of the system of interest, and the time correlation function between two operators  $\hat{A}$  and  $\hat{B}$  for a time-independent Hamiltonian  $\hat{H}$  is given by

$$C_{AB}(t) \equiv \text{Tr}[\hat{\rho}_0 \hat{A} \hat{B}(t)] = \int dx_t \langle \varphi_0 | x_t \rangle A(x_t) \langle x_t | e^{i\hat{H}t/\hbar} \hat{B} | \varphi_0 \rangle e^{-iE_0 t/\hbar}, \quad (2.13)$$

where  $E_0$  is the ground state energy eigenvalue. In many applications, the correlation function of interest is obtained with  $\hat{A} = \hat{B} = \hat{x}$  (the leading term of the dipole moment operator for vibrational transitions) or  $\hat{A} = \hat{B} = \hat{p}$  (velocity autocorrelation function). Notice that the evolution of the system forward to time  $+t$  has been carried out analytically, and the remaining task is to evaluate the backward propagation of the Bohmian swarm by  $-t$ , starting with the “initial” state,

$$\Psi_B(x, 0) = \langle x | \hat{B} | \varphi_0 \rangle, \quad (2.14)$$

i.e., to determine

$$\Psi_B(x, -t) \equiv \langle x | e^{i\hat{H}t/\hbar} \hat{B} | \varphi_0 \rangle \quad (2.15)$$

from the quantum trajectories using Eq. (2.11).

In the special case of a harmonic potential  $V_{\text{cl}}$ , when  $\hat{B} = \hat{x}$  (or  $\hat{p}$ ), the state  $\Psi_B$  is also an energy eigenstate (up to a constant multiplicative factor), and the backward evolution can also be carried out analytically. For bound, mildly anharmonic systems,  $|\Psi_B(0)\rangle = \hat{x} |\varphi_0\rangle$  closely resembles an energy

eigenstate, in general (and the same holds for  $\hat{p}|\varphi_0\rangle$ ). As a result, the quantum potential and the trajectories for the backward evolution are much more slowly varying and better behaved than when starting from other initial states.<sup>28</sup>

Due to sensitivity to numerical error, direct integration of Eq. (2.7) and coevolution of the time-dependent density have not met with practical success for general anharmonic systems without additional input, even if one starts from the favorable initial state  $\hat{x}|\varphi_0\rangle$  or  $\hat{p}|\varphi_0\rangle$ .

### III. TIME CORRELATION FUNCTIONS VIA QUANTUM TRAJECTORIES FROM HAMILTON'S LAW

#### A. Time-dependent Jacobian

The time-dependent density can be obtained from the continuity equation,

$$\rho(x_t, t) = J_t(x_t)\rho(x_0, 0), \quad (3.1)$$

where

$$J_t = \frac{\partial x_0}{\partial x_t} \quad (3.2)$$

is the time-dependent Jacobian, which will now be cast as the central dynamical quantity. Through repeated use of the chain rule identity  $\partial/\partial x_t = J_t \partial/\partial x_0$ , it is tedious but straightforward to obtain the quantum potential and force in terms of  $J_t$  and zero-time quantities,

$$V_{\text{qm}}(x_t, t) = J_t^2 V_{\text{qm}}(x_0, 0) - \frac{\hbar^2}{2m} \left[ \frac{J_t''}{2J_t} - \frac{J_t'^2}{4J_t^2} + J_t' \frac{\rho_0'}{\rho_0} \right], \quad (3.3)$$

$$\begin{aligned} \frac{\partial V_{\text{qm}}(x_t, t)}{\partial x_t} &= J_t^3 \frac{\partial V_{\text{qm}}(x_0, 0)}{\partial x_0} - \frac{\hbar^2}{2m} \left[ \frac{J_t'''}{2J_t} - \frac{J_t' J_t''}{J_t^2} + \frac{J_t'^3}{2J_t^3} \right. \\ &\quad \left. + 2J_t J_t' \left( \frac{\rho_0''}{\rho_0} - \frac{3\rho_0'^2}{4\rho_0^2} \right) + J_t'' \frac{\rho_0'}{\rho_0} \right], \end{aligned} \quad (3.4)$$

where  $\rho_0' \equiv \partial\rho(x_0, 0)/\partial x_0$ ,  $J_t' \equiv \partial J_t/\partial x_t$ , etc. The point of Eqs. (3.3) and (3.4) is to take advantage of the zero-time quantum potential, force, and density, all of which can be obtained very accurately from the ground state wavefunction (multiplied by  $x$  or  $p$ ). Also, since spatial derivatives at nonzero times are computed on the coarse, time-dependent grid formed by the trajectories themselves, it is beneficial to restrict all occurrences of  $\partial/\partial x_t$  to the Jacobian, which generally is a smooth quantity in FBQD.

As a time-dependent quantity, the Jacobian field itself must be inferred from the dynamical information contained within the quantum trajectories. For instance, if the velocity field  $v_t(x_t)$  is available, then the Jacobian  $J_t$  can be obtained as<sup>32</sup>

$$J_t = \exp\left(-\int_0^t \frac{\partial v_{t'}}{\partial x_{t'}} dt'\right). \quad (3.5)$$

#### B. Quantum potential near nodes

The numerical difficulties associated with nodes in Bohm's formulation have been discussed extensively.<sup>32</sup> When the wavefunction density is zero, evaluation of the quantum potential via Eq. (2.9) is problematic, with the quantum potential and resulting trajectories in most cases undergoing extremely rapid variations that lead to instabilities. These behaviors occur primarily in regions of strong quantum interference, where classical trajectories cross and the semiclassical wavefunction encounters caustics.<sup>33</sup>

We note here, however, that a wavefunction node does not necessarily cause the quantum potential to diverge. For example, with eigenstates of the Hamiltonian, the second derivative of the wavefunction  $\psi(x)$  must vanish at points of zero density, so nodes are also inflection points. Thus the numerator in Eq. (2.9) is also equal to zero, and the wavefunction at a node located at  $a$  can be written as  $\psi(x) = (x-a)f(x)$ . Application of l'Hospital's rule gives

$$V_{\text{qm}}(a) = -\frac{\hbar^2}{2m} \frac{\psi'''(a)}{\psi'(a)} = -\frac{\hbar^2}{2m} \frac{3f''(a)}{f(a)}, \quad (3.6)$$

where we have allowed  $R < 0$  in Eq. (2.2) to permit differentiation where  $\psi$  changes sign. Note that this does not affect our final wavefunction (2.11), which is defined in terms of  $\rho \equiv R^2$ . Thus, the apparent singularity in the determination of the quantum potential is removable, as long as  $f(a)$ ,  $f''(a) \neq 0$ . This procedure is applicable to more general situations, provided the second derivative of the amplitude vanishes at the node (a necessary condition for a finite quantum potential when  $\psi=0$ ).

Implementation of this technique to ameliorate numerical problems associated with nodes is straightforward in the present treatment, where the quantum potential and force are calculated in terms of the initial density and its derivatives. First, we note that the FBQD wavefunction in Eq. (2.14) must have an inflection point at a node in order for the quantum potential to be finite. For  $\hat{B} = \hat{x}$ , the initial wavefunction for the backward propagation is  $x\varphi_0(x)$ , which (unless the maximum of  $|\varphi_0|$  is at  $x=0$ ) will not satisfy the above requirement, leading to infinite quantum potential at the node. To remedy this situation, we write the position correlation function in the form

$$C_{xx}(t) \equiv \langle \hat{x}\hat{x}(t) \rangle = \langle \hat{x} e^{iHt/\hbar} (\hat{x} - x_{\text{peak}}) e^{-iHt/\hbar} \rangle + \langle \hat{x} \rangle x_{\text{peak}}, \quad (3.7)$$

where  $x_{\text{peak}}$  is the coordinate of the maximum of the ground state wavefunction. The second term on the right hand side is proportional to a simple zero-time expectation value. The first term is the correlation function for a shifted operator,  $\hat{B} = \hat{x} - x_{\text{peak}}$ , which can be obtained through a zero-temperature FBQD simulation, where the backward propagation now starts from the modified initial state,

$$|\Psi_B(t=0)\rangle = (\hat{x} - x_{\text{peak}})|\varphi_0\rangle. \quad (3.8)$$

By construction, the node of Eq. (3.8) is also an inflection point, allowing the zero-time quantum potential to be evaluated using l'Hospital's rule as described above.

### C. Hamilton's law of varying action

As stated in Sec. I, conventional algorithms for solving Bohm's differential equations generally are not successful when applied to bound anharmonic systems. To improve stability, we seek an algorithm that is global in time. A useful application of such methods is in the search for classical paths connecting important points (e.g., transition states or local minima) of a potential energy surface.

The best known form of Hamilton's principle involves variation with fixed endpoints,  $\delta x(t_0) = \delta x(t_F) = 0$ . In this special case, Hamilton's postulate states that

$$\delta S = \int_{t_0}^{t_F} [m\dot{x}(t)\delta\dot{x}(t) - V'(x(t))\delta x(t)]dt = 0, \quad (3.9)$$

where  $\delta x(t)$  is an infinitesimal virtual displacement and  $\delta\dot{x}(t)$  denotes its time derivative. Since Bohm's quantum trajectories obey classical-like equations of motion with a modified potential, these trajectories must also satisfy Hamilton's variational principle when boundary conditions are prescribed on initial and final trajectory positions. However, the quantum trajectories we seek are specified from the initial conditions  $x_0$  and  $m\dot{x}_0 = S'_0(x_0)$  [Eq. (2.12)], rather than fixed boundary conditions.

We thus need to resort to a more general variational equation, often referred to as Hamilton's law of varying action<sup>29,30,34,35</sup> (HLVA), which states

$$\delta S = \int_{t_0}^{t_F} [m\dot{x}(t)\delta\dot{x}(t) - V'(x(t))\delta x(t)]dt = m\dot{x}(t)\delta x(t)|_{t_0}^{t_F}. \quad (3.10)$$

This law specifies the classical path of the system subject to general boundary conditions and thus can be applied to Bohm's equations with the specified initial conditions. With simple manipulations, Eq. (3.10) leads to the Euler-Lagrange equation of motion for the trajectory, with arbitrary boundary conditions. Note that  $\delta S \neq 0$ , in general. With fixed endpoint boundary conditions, Eq. (3.10) reverts to the more familiar Eq. (3.9).

Interestingly, for a real-valued initial wavefunction, Eq. (2.12) implies  $\dot{x}(t_0) = 0$ . With this so-called natural boundary condition at  $t = t_0$  and the additional boundary condition  $\delta x(t_F) = 0$ , the right hand side of Eq. (3.10) vanishes, allowing us to apply the principle of stationary action to Bohm's equations. In a variational procedure, this is accomplished by initializing a trajectory with fixed final position  $x(t_F)$ , then varying the trajectory at all times except  $t_F$  until the action integral is stationary, allowing free variation of the initial position  $x(t_0)$  to "enforce" the natural boundary condition.<sup>36</sup>

Indeed, our original line of approach was to expand  $x(t)$  as a truncated Fourier cosine series satisfying these mixed boundary conditions. However, this boundary value problem (BVP) was not as flexible as the initial value problem (IVP) described below. First, this BVP formulation requires a real-valued initial wavefunction, whereas the IVP does not. Second, the BVP by nature can only be solved for one time interval  $\Delta t \equiv t_F - t_0$ , with longer time accessible only by increasing  $\Delta t$  and, consequently, the required number of Fou-

rier coefficients. This is because once the BVP has been solved, trajectory positions and momenta are fully specified everywhere on the time interval, and the latter generally will not vanish for all trajectories at  $t_0 + \Delta t$ . The IVP, on the other hand, can be iterated repeatedly with smaller  $\Delta t$ , keeping the number of unknown coefficients small in each iteration. Third, because solving the BVP is an "all-or-nothing" procedure, several separate runs are required to determine how large  $t_F$  can be made before the solver starts to break down. By iterating the IVP, on the other hand, the gradual breakdown of the solver can be observed from a single simulation.

### D. Solution of the initial value HLVA problem

This section describes a solution of HLVA (3.10) subject to the initial conditions

$$x(t_0) = x_0, \quad p(t_0) = p_0. \quad (3.11)$$

The overall strategy, originated by Bailey,<sup>34,35</sup> is an adaptation of the Galerkin procedure<sup>36,37</sup> for solving BVPs for integral representations of ordinary and partial differential equations. Specifically, the trajectories and virtual displacements are expanded in truncated series in time, using HLVA, Eq. (3.10), to determine the expansion coefficients. We considered and tried various forms for this task, including Taylor, Fourier, and Chebychev series, as well as a finite element representation. Time finite element expansions are known to encounter convergence problems,<sup>38</sup> as well as an undesirable, unavoidable coupling of the number of unknown coefficients to the refinement of the time quadrature in Eq. (3.10). In order to enforce the initial conditions, linear dependence must be introduced between the coefficients of Fourier and Chebychev expansions; when applied to FBQD, we found the latter to be costlier and no more accurate or stable than the simple Taylor expansion, which we now consider exclusively. Alternate expansions may prove useful for generalizing this method to less stationary wavefunctions [e.g., Fig. 3(b)], although in such cases, the problem of obtaining accurate spatial derivatives for Eq. (3.4) must first be solved.

Following Bailey,<sup>34,35</sup> the trajectory  $x(\tau)$  and virtual displacement  $\delta x(\tau)$  are expanded as power series in the dimensionless reduced time  $\tau \equiv (t - t_0)/(t_F - t_0)$ ,

$$x(\tau) = x_0 + m^{-1}p_0(t_F - t_0)\tau + \sum_{k=2}^N c_k \tau^k, \quad (3.12)$$

$$\delta x(\tau) = \sum_{k=2}^N \tau^k \delta c_k, \quad (3.13)$$

where  $\delta c_0$  and  $\delta c_1$  must vanish for the virtual displacement  $\delta x$  to satisfy the prescribed initial conditions. Since  $d\tau/dt = (t_F - t_0)^{-1}$ ,

$$\begin{aligned} \dot{x}(\tau) &\equiv \frac{dx}{dt} = (t_F - t_0)^{-1} \frac{d}{d\tau} x(\tau) \\ &= m^{-1}p_0 + (t_F - t_0)^{-1} \sum_{k=2}^N k c_k \tau^{k-1}, \end{aligned} \quad (3.14)$$

$$\delta\dot{x}(\tau) = (t_F - t_0)^{-1} \frac{d}{d\tau} \delta x(\tau) = (t_F - t_0)^{-1} \sum_{k=2}^N k \tau^{k-1} \delta c_k. \quad (3.15)$$

Substituting Eqs. (3.12)–(3.15) into Hamilton's law, Eq. (3.10), and integrating the kinetic term gives

$$0 = \sum_{k=2}^N \delta c_k \left[ \frac{m}{t_F - t_0} \sum_{j=2}^N \frac{j(j-1)}{k+j-1} c_j + (t_F - t_0) \times \int_0^t \frac{\partial V(x(\tau))}{\partial x} \tau^k d\tau \right]. \quad (3.16)$$

Because Eq. (3.16) must hold for all admissible virtual displacements (i.e., for arbitrary  $\delta c_k$ ), the quantity in square brackets must vanish, yielding

$$0 = \frac{m}{t_F - t_0} \sum_{j=2}^N \frac{j(j-1)}{k+j-1} c_j + (t_F - t_0) \int_0^t \frac{\partial V(x(\tau))}{\partial x} \tau^k d\tau, \quad (3.17)$$

$$k = 2, \dots, N.$$

Note that Eq. (3.17) is equally applicable in the classical and quantum cases; for the latter, the difficulty is in the accurate determination of the quantum force  $-\partial V_{\text{qm}}/\partial x$ .

Equation (3.17) can also be derived from the weak form of the differential equation,

$$\int_{t_0}^{t_F} [m\ddot{x} + V'(x(t))]w(t)dt = 0, \quad (3.18)$$

where  $w(t)$  is an arbitrary weight function and two of the four quantities  $w(t_0)$ ,  $\dot{w}(t_0)$ ,  $w(t_F)$ ,  $\dot{w}(t_F)$ , are prescribed to vanish.<sup>39</sup> If  $w(t_0) = \dot{w}(t_0) = 0$ , then  $x(t)$  and  $x(t) + w(t)$  both satisfy the initial conditions (3.11), and Eq. (3.18) is a variational equation as written in Eq. (3.10). However, if any other two quantities are chosen to vanish, the resulting weighted residual scheme cannot be interpreted as an application of the calculus of variations. This is precisely the distinction between the Galerkin and Petrov–Galerkin procedures.<sup>36</sup> In the present application to FBQD, we have observed Petrov–Galerkin and collocation-based schemes to be no more accurate and significantly less stable than the simple Galerkin formulation, Eq. (3.17).

### E. Application to quantum trajectories

The dynamical problem is thus reduced to the determination of the unknown coefficients  $c_k$  in expansion (3.12). For the FBQD problem, the evolution of each of the  $n$  particles in the Bohmian fluid is governed by  $N-1$  equations of the form (3.17). Due to the nonlocal nature of the quantum force (3.4), these  $n(N-1)$  coupled nonlinear equations must be solved simultaneously. In the examples below this is accomplished using a simple quasi-Newton subroutine.<sup>40</sup>

In the Bohmian case, the total potential energy of a particle is  $V(x,t) = V_{\text{cl}}(x) + V_{\text{qm}}(x,t)$ , so all that remains is to evaluate the quantum force in Eq. (3.17). As mentioned in Sec. III A, aside from zero-time information, the time-dependent Jacobian  $J_t$  and its spatial derivatives suffice to

determine the quantum force via Eq. (3.4), while zero-time quantities such as  $\rho_0$  and  $V_{\text{qm}}(x_0, 0)$  can be computed accurately by diagonalization of the Hamiltonian matrix or similar methods.

In the examples that follow, Eq. (3.17) was solved simultaneously for a “swarm” of  $n \approx 50$  Bohmian trajectories, obtaining  $J_t$  through Eq. (3.5) and its spatial derivatives by finite difference. The initial state for the Bohmian propagation was Eq. (3.8), and in each iteration (time interval  $\Delta t = t_F - t_0$ ) of Eq. (3.17), trajectories were initialized to straight-line trial forms. For each particle in the fluid, the initial position  $x_0$  in Eq. (3.11) was chosen arbitrarily, and the initial momentum (3.11) was initialized to  $p_0 = 0$  [again, by merit of Eqs. (2.5) and (2.2) applied to the real-valued initial state created by the action of the operator  $\hat{B}$ , or its shifted form, on the ground state wavefunction].

Spatial derivatives at nonzero time were computed using three-point finite difference formulas, with higher-order derivatives taken by successive differentiation. Four- and five-point formulas were not found to give improved results. It was also found to be important to include trajectories from both sides of the node at  $x_0 = x_{\text{peak}}$  in the computation of spatial derivatives in order to obtain accurate results at long time. Application of l'Hospital's rule was only implemented for the zero-time quantum potential; nodes at nonzero time were in some sense “ignored.” For instance, in the case of symmetric potentials with  $x_{\text{peak}} = 0$  in Eq. (3.8), spatial derivatives [e.g., the velocity field in Eq. (3.5)] were taken by simple finite difference using function values on either side of  $x_t = 0$ , and this simple treatment yielded satisfactory results.

### IV. NUMERICAL EXAMPLES

The examples below illustrate the method described in the previous sections for computing FBQD trajectories and the corresponding correlation functions for one-dimensional oscillators. For both examples, the particle was assigned unit mass, time interval  $\Delta t = 2$ ,  $dt = 0.05$  for the time quadrature in Eq. (3.10), the spatial grid extended between  $x_{\text{peak}} \pm 3$  with initial particle spacing  $\Delta x_0 = 0.1$ , and the Taylor series order was  $N = 4$  (i.e., three unknown  $c_j$  per particle were used in each time interval). To avoid numerical problems associated with nodes at nonzero time in the backward evolution, no particles were initialized in the interval between  $x_{\text{peak}} \pm 0.1$ . For both of the models described below we evaluate the position correlation function setting  $\hat{A} = \hat{x}$  and  $\hat{B} = \hat{x} - x_{\text{peak}}$  in Eq. (2.13). For comparison, exact results for the quantum trajectories and the correlation function were obtained from the exact solution to the Schrödinger equation, obtained with the split operator method.<sup>41</sup>

First consider a purely anharmonic oscillator with potential energy given by

$$V_{\text{cl}}(x) = \frac{1}{4}x^4, \quad (4.1)$$

which is expected to be a challenging system based on the discussion in Sec. II C. Indeed, we are not aware of any method that can obtain quantum trajectories for this potential without input obtained from *a priori* knowledge of the exact

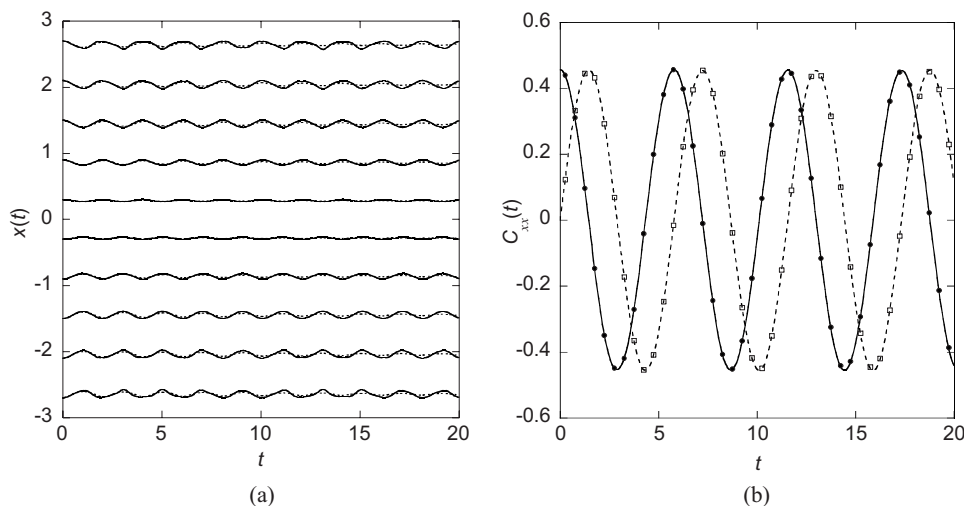


FIG. 1. (a) Selected quantum trajectories, approximate (dashed) and exact (solid), respectively, obtained from the HLVA solver described in Sec. III and the time-dependent density from a separate split-operator calculation (Ref. 41). (b) Zero-temperature FBQD position autocorrelation function for the symmetric quartic oscillator described by Eq. (4.1). Filled circles and hollow squares show real and imaginary parts, respectively. For comparison, the solid and dashed lines display the exact result.

solution. As seen in Fig. 1(a), the method introduced in Sec. III produces stable trajectories, although high accuracy is achieved only during the initial two to three oscillations and the trajectories damp out to a mean position at long times. In spite of these deviations from the exact quantum trajectories, the resulting position correlation function shown in Fig. 1(b) remains accurate even at long time, after the HLVA solver has “overdamped” the approximate trajectories. This indicates that for this system, after the short time action has been computed to reasonable accuracy,  $V(\bar{x})\Delta t$  is a satisfactory approximation for subsequent contributions to the action integral, where  $\bar{x}$  is the “damped” final position of the particle. In this and the next example, taking a smaller time interval  $\Delta t=1$  resulted in less “damping” and more accurate trajectories, but also decreased the stability of the simulation without increasing the accuracy of the correlation function. It is interesting to note that the damped density inferred from the approximate HLVA trajectories was found to approach the excited state density, instead of continuing to oscillate about the latter. This behavior was found to emerge naturally from the HLVA procedure.

Next, consider a strongly anharmonic oscillator with potential energy function,

$$V_{\text{cl}}(x) = \frac{1}{2}x^2 - 0.1x^3 + 0.1x^4. \quad (4.2)$$

Even though this system contains a quadratic term and thus is less anharmonic than the first model, it presents a greater challenge to our method. As seen in Fig. 2(a), the approximate quantum trajectories resemble those obtained for the quartic oscillator in Fig. 1(a), but become progressively less accurate as Bohmian particles are placed closer to the node. The exact trajectories of such particles undergo sharp turns that are not reproduced by the HLVA solver. The source of this behavior is the spatial asymmetry caused by the cubic term in Eq. (4.2). This asymmetry causes the density to slosh back and forth across the initial node position, a behavior which our HLVA solver is unable to capture, not only due to the low order of our Taylor expansion but also because the massive density fluctuations make it difficult to accurately compute the multiple spatial derivatives required by Eq. (3.4).

Figure 2(b) shows that the position correlation function obtained from the HLVA quantum trajectories decays slightly in amplitude at long time, although the frequency of oscillation is well preserved. Nevertheless, the correlation function remains highly accurate for the first three oscillation periods, in spite of the qualitatively incorrect behavior of the approxi-

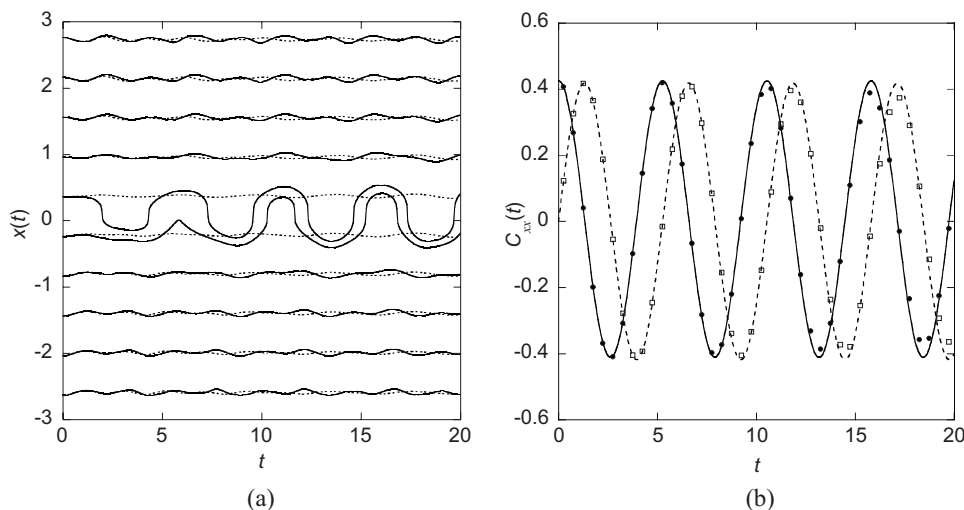


FIG. 2. (a) Selected Bohmian trajectories, approximate (dashed) and exact (solid), respectively, obtained from the HLVA solver described in Sec. III and the time-dependent density from a separate split-operator calculation (Ref. 41). The spatial asymmetry resulting from the cubic term in Eq. (4.2) induces particles to cross the initial node position  $x_{\text{peak}}=0.062$ . (b) Zero-temperature FBQD position autocorrelation function for the asymmetric oscillator described by Eq. (4.2). Filled circles and hollow squares show real and imaginary parts, respectively. For comparison, the solid and dashed lines display the exact result.

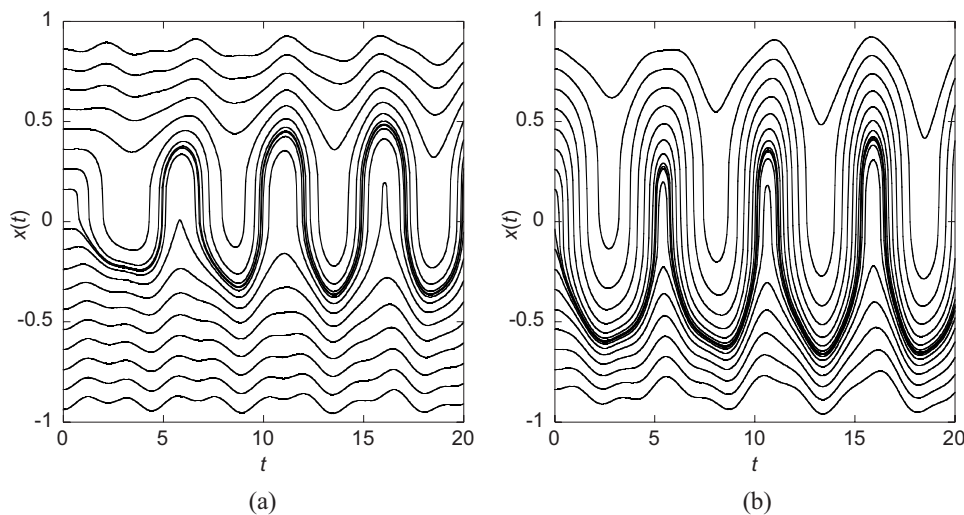


FIG. 3. Exact FBQD trajectories for the asymmetric oscillator (4.2) obtained from a split-operator calculation, with initial wavefunction (a)  $(x - x_{\text{peak}})\varphi_0(x)$  and (b)  $x\varphi_0(x)$ , where  $x_{\text{peak}} \approx 0.062$  is the location of the maximum in the ground state wavefunction  $\varphi_0(x)$ . In the first case, the zero-time quantum potential at the node is obtained using l'Hospital's rule as described in Sec. III B and has a finite value, leading to smoother quantum trajectories.

mate trajectories in the vicinity of the wavefunction node. This occurs because the total amount of density that crosses the initial node position is not large, so its inadequate description does not significantly affect the value of the integral in Eq. (2.13). The particles that lie farther from the node and are responsible for the bulk of the integral in Eq. (2.13) are in much better agreement with the exact trajectories, thus leading to an accurate evaluation of the correlation function.

Figure 3 shows a more detailed view of the exact quantum trajectories near the origin. Figure 3(a) is just a reproduction of the exact trajectories in Fig. 2(a) at a finer  $\Delta x_0$  resolution, showing trajectories obtained by shifting the operator  $\hat{B}$  to place the node at an inflection point as described in the discussion preceding Eq. (3.8). In comparison, the exact quantum trajectories in Fig. 3(b) were obtained from the naively selected initial wavefunction  $x\varphi_0(x)$ . It is clear that the trajectories are much smoother in the former case, a consequence of removing the singularity from the zero-time quantum potential. Solving the HLVA equations (3.17) with the latter initial condition did not yield an accurate correlation function even at short time  $t=1$  (not shown). Also, when the asymmetric term in Eq. (4.2) is increased further, our HLVA solver breaks down even for  $(x - x_{\text{peak}})\varphi_0(x)$ , which becomes an increasingly poor approximation to the first excited state. Allowing the coordinate shift  $x_{\text{peak}}$  to vary with time according to a zeroth order approximate form<sup>42</sup> may improve stability in such situations.

## V. CONCLUDING REMARKS

In this paper we have presented a numerical methodology for determining quantum trajectories in bound anharmonic systems. To avoid numerical instabilities arising from the use of the instantaneous quantum force to propagate a trajectory forward in time, our procedure employs a time series representation of the trajectory and uses HLVA to determine the expansion coefficients. Further, our method evaluates the quantum potential in terms of the initial density and the time-dependent Jacobian, allowing application of l'Hospital's rule to eliminate singularities of the zero-time quantum potential at nodes if the second derivative of the wavefunction vanishes.

We showed that the HLVA procedure can be successfully applied to the FBQD formulation of zero-temperature time correlation functions. Because the action of common (position or momentum) operators on the ground state of a bound system produces a near eigenstate, the quantum potential is smooth and the corresponding quantum trajectories are generally well behaved. The HLVA procedure led to stable and accurate results for the position autocorrelation functions in two strongly anharmonic oscillators. Bohmian trajectories for nonstationary states in bound anharmonic systems have been obtained by other methods,<sup>20,43–46</sup> but only for a very weakly anharmonic potential, or with the addition of stabilizing terms to the algorithm. The approach described in this paper was able to handle a quartic potential with zero harmonic component, making no additional assumptions beyond those intrinsic to numerical solution of Hamilton's law. The feasibility of our approach relies on the near stationarity of the initial wavefunction. To our knowledge, this is the first calculation of a time correlation function in a bound strongly anharmonic system exclusively using Bohm's formulation of quantum mechanics.

In the current implementation of our method, it was assumed that the trajectory can be accurately treated by a low order power series expansion in time and that spatial derivatives can be accurately obtained by finite difference on the trajectory grid. Stability and accuracy thus depend on the judicious selection of a sufficiently stationary initial wavefunction, which was accomplished in this paper through a minor modification of the FBQD prescription. When the initial FBQD wavefunction is highly nonstationary, the time-dependent Jacobian becomes spatially rugged and its derivatives become difficult to obtain accurately by finite difference; it remains to be seen whether more sophisticated differentiation algorithms would remedy this shortcoming. Moreover, due to the need to solve a system of coupled nonlinear equations whose size is proportional to the number of expansion coefficients, the approach explored in this paper is best suited to slowly varying trajectories which are amenable to a low-order expansion. While this is indeed the case with some zero-temperature FBQD trajectories, it is unclear whether the HLVA approach would be feasible with more general initial wavefunctions. Also, because our method de-

termines all trajectories in the discretized Bohmian fluid simultaneously, an exact generalization to higher dimensional systems will exhibit exponential scaling in the grid formed by the trajectories. Whether a quantum-classical scheme that avoids this unfavorable scaling can be formulated is currently being investigated.

## ACKNOWLEDGMENTS

This material is based on work supported by the National Science Foundation under Award Nos. ITR 04-27082, CHE 05-18452, and CHE 08-09699. Calculations were performed on a Linux cluster acquired through CRIF 05-41659. J.C. is grateful for an Illinois Distinguished Fellowship and a Victor E. Buhrke Fellowship.

<sup>1</sup>L. de Broglie, C. R. Hebd. Seances Acad. Sci. **183**, 447 (1926).

<sup>2</sup>E. Madelung, Z. Phys. **40**, 322 (1926).

<sup>3</sup>D. Bohm, Phys. Rev. **85**, 166 (1952).

<sup>4</sup>D. Bohm, Phys. Rev. **85**, 180 (1952).

<sup>5</sup>B. K. Dey, A. Askar, and H. Rabitz, J. Chem. Phys. **109**, 8770 (1998).

<sup>6</sup>C. L. Lopreore and R. E. Wyatt, Phys. Rev. Lett. **82**, 5190 (1999).

<sup>7</sup>F. S. Mayor, A. Askar, and H. A. Rabitz, J. Chem. Phys. **111**, 2423 (1999).

<sup>8</sup>R. E. Wyatt, Chem. Phys. Lett. **313**, 189 (1999).

<sup>9</sup>E. R. Bittner, J. Chem. Phys. **112**, 9703 (2000).

<sup>10</sup>R. E. Wyatt, D. J. Kouri, and D. K. Hoffman, J. Chem. Phys. **112**, 10730 (2000).

<sup>11</sup>C. L. Lopreore and R. E. Wyatt, Chem. Phys. Lett. **325**, 73 (2000).

<sup>12</sup>D. Nerukh and J. H. Frederick, Chem. Phys. Lett. **332**, 145 (2000).

<sup>13</sup>R. E. Wyatt and E. R. Bittner, J. Chem. Phys. **113**, 8898 (2000).

<sup>14</sup>O. V. Prezhdo and C. Brooksby, Phys. Rev. Lett. **86**, 3215 (2001).

<sup>15</sup>Z. S. Wang, G. R. Darling, and S. Holloway, J. Chem. Phys. **115**, 10373 (2001).

<sup>16</sup>J. B. Maddox and E. R. Bittner, J. Chem. Phys. **115**, 6309 (2001).

<sup>17</sup>I. Burghardt and L. S. Cederbaum, J. Chem. Phys. **115**, 10303 (2001).

<sup>18</sup>J. B. Maddox and E. R. Bittner, Phys. Rev. E **65**, 026143 (2002).

<sup>19</sup>R. E. Wyatt and K. Na, Phys. Rev. E **65**, 016702 (2002).

<sup>20</sup>R. E. Wyatt, J. Chem. Phys. **117**, 9569 (2002).

<sup>21</sup>Y. Zhao and N. Makri, J. Chem. Phys. **119**, 60 (2003).

<sup>22</sup>J. Liu and N. Makri, J. Phys. Chem. A **108**, 5408 (2004).

<sup>23</sup>B. Poirier, J. Chem. Phys. **121**, 4501 (2004).

<sup>24</sup>J. Liu and N. Makri, Mol. Phys. **103**, 1083 (2005).

<sup>25</sup>Y. Goldfarb, I. Degani, and D. J. Tannor, J. Chem. Phys. **125**, 231103 (2006).

<sup>26</sup>Y. Goldfarb and D. J. Tannor, J. Chem. Phys. **127**, 161101 (2007).

<sup>27</sup>Y. Goldfarb, J. Schiff, and D. J. Tannor, J. Phys. Chem. A **111**, 10416 (2007).

<sup>28</sup>N. Makri, J. Phys. Chem. A **108**, 806 (2004).

<sup>29</sup>W. R. Hamilton, Philos. Trans. R. Soc. London **125**, 95 (1835).

<sup>30</sup>W. R. Hamilton, Philos. Trans. R. Soc. London **124**, 247 (1834).

<sup>31</sup>W. Yourgrau and S. Mandelstam, *Variational Principles in Dynamics and Quantum Theory* (Dover, New York, 1979).

<sup>32</sup>R. E. Wyatt, *Quantum Dynamics with Trajectories* (Springer, New York, 2005).

<sup>33</sup>L. S. Schulman, *Techniques and Applications of Path Integration* (Wiley, New York, 1981).

<sup>34</sup>C. D. Bailey, AIAA J. **13**, 1154 (1975).

<sup>35</sup>C. D. Bailey, Found. Phys. **5**, 433 (1975).

<sup>36</sup>O. Axelsson and V. A. Barker, *Finite Element Solution of Boundary Value Problems* (SIAM, Philadelphia, 2001).

<sup>37</sup>M. T. Heath, *Scientific Computing* (McGraw-Hill, Boston, 2002).

<sup>38</sup>T. E. Simkins, AIAA J. **19**, 1357 (1981).

<sup>39</sup>M. Baruch and R. Riff, AIAA J. **20**, 687 (1982).

<sup>40</sup>C. G. Broyden, Math. Comput. **19**, 577 (1965).

<sup>41</sup>M. D. Feit, J. A. J. Fleck, and A. Steiger, J. Comput. Phys. **47**, 412 (1982).

<sup>42</sup>S. Garashchuk and V. A. Rassolov, J. Chem. Phys. **121**, 8711 (2004).

<sup>43</sup>E. R. Bittner, J. Chem. Phys. **119**, 1358 (2003).

<sup>44</sup>V. A. Rassolov and S. Garashchuk, J. Chem. Phys. **120**, 6815 (2004).

<sup>45</sup>S. Garashchuk and V. A. Rassolov, J. Phys. Chem. A **111**, 10251 (2007).

<sup>46</sup>S. Garashchuk and V. A. Rassolov, J. Chem. Phys. **129**, 024109 (2008).